The Astrophysical Journal Letters, 741:L37 (6pp), 2011 November 10 doi:10.1088/2041-8205/741/2/L37

THE WATER VAPOR SPECTRUM OF APM 08279+5255: X-RAY HEATING AND INFRARED PUMPING OVER HUNDREDS OF PARSECS

C. M. Bradford[1,2], A. D. Bolatto[3], P. R. Maloney[4], J. E. Aguirre[4,5], J. J. Bock[1,2], J. Glenn[4], J. Kamenetzky[4], R. Lupu[5], H. Matsuhara[6], E. J. Murphy[7], B. J. Naylor[1,2], H. T. Nguyen[1], K. Scott[5], and J. Zmuidzinas[1,2]
[1] Jet Propulsion Laboratory, California Institute of Technology, Pasadena, CA 91109, USA
[2] California Institute of Technology, Pasadena, CA 91125, USA
[3] Department of Astronomy, University of Maryland, College Park, MD 20742-2421, USA
[4] Center for Astrophysics and Space Astronomy, University of Colorado, Boulder, CO 80303, USA
[5] Department of Physics, University of Pennsylvania, Philadelphia, PA 19104, USA
[6] Institute for Space and Astronautical Science, Japan Aerospace and Exploration Agency, 3-1-1 Yoshinodai, Chuo-ku, Sagamihara 252-5210, Japan
[7] Observatories of the Carnegie Institution for Science, 813 Santa Barbara Street, Pasadena, CA 91101, USA
Received 2011 June 21; accepted 2011 July 13; published 2011 October 21

ABSTRACT

We present the rest-frame 200–320 μm spectrum of the $z = 3.91$ quasar APM 08279+5255, obtained with Z-Spec at the Caltech Submillimeter Observatory. In addition to the $J = 8 \rightarrow 7$ to $J = 13 \rightarrow 12$ CO rotational transitions which dominate the CO cooling, we find six transitions of water originating at energy levels ranging up to 643 K. Most are first detections at high redshift, and we have confirmed one transition with CARMA. The CO cooling is well described by our X-ray dominated region (XDR) model, assuming $L_{1-100\,\mathrm{keV}} \sim 1 \times 10^{46}$ erg s^{-1}, and that the gas is distributed over a 550-pc size scale, as per the now-favored $\mu = 4$ lensing model. The total observed cooling in water corresponds to $6.5 \times 10^9\ L_\odot$, comparable to that of CO. We compare the water spectrum with that of Mrk 231, finding that the intensity ratios among the high-lying lines are similar, but with a total luminosity scaled up by a factor of ~50. Using this scaling, we estimate an average water abundance relative to H_2 of 1.4×10^{-7}, a good match to the prediction of the chemical network in the XDR model. As with Mrk 231, the high-lying water transitions are excited radiatively via absorption in the rest-frame far-infrared, and we show that the powerful dust continuum in APM 08279+5255 is more than sufficient to pump this massive reservoir of warm water vapor.

Key words: galaxies: active – instrumentation: spectrographs – ISM: molecules – quasars: emission lines

Online-only material: color figures

1. INTRODUCTION

1.1. Water as a Molecular Gas Coolant and Radiation Field Probe

Though virtually impossible to observe in the local universe from the ground, H_2O is an important constituent of interstellar gas under the right conditions. The species is chemically enhanced for temperatures above a few hundred Kelvin (Draine & Roberge 1982), and is sublimated from grain mantles as dust is heated to ~100 K. It then becomes an important gas-phase repository for oxygen, with abundance approaching that of CO (e.g., Cernicharo et al. 2006). With water's large dipole moment, the network of rotational transitions can either be a dominant molecular coolant (for $T > 300$ K and $n_{H_2} > 10^5$cm^{-3}; Hollenbach & McKee 1979; Neufeld & Melnick 1987; Neufeld & Kaufman 1993, and references therein), or a pathway for coupling mid- and far-infrared continuum radiation into the gas if the local continuum is sufficiently strong (e.g., Scoville & Kwan 1976).

Many of the most important H_2O transitions lie in the short submillimeter between 200 and 300 μm, which has until recently been inaccessible in the local universe and only sparsely explored at high redshifts via observations in the millimeter band. With the advent of broadband spectrometers enabled by high-performance bolometer arrays (Herschel SPIRE—Griffin et al. 2010; Z-Spec—e.g., Earle et al. 2006), the water spectrum can be explored on galaxy scales locally and at high redshift. Water is not an important coolant in the overall energy budget of the gas in the Milky Way (via *COBE*; Fixsen et al. 1999) or even in the nucleus of the nearby starburst galaxy M82 (Panuzzo et al. 2010). However, in extreme ULIRGs such as Arp 220 (Rangwala et al. 2011) and Mrk 231 (van der Werf et al. 2010, hereafter vdW10; González-Alfonso et al. 2010, hereafter GA10), the most luminous H_2O transitions can be comparable in strength to those of CO.

Through comparison with water excitation models, GA10 show that the water emission lines in Mrk 231 measured with SPIRE are not produced by purely collisional excitation; the ratio of high-level transitions to the lower level and ground-state transitions is too large, even for shock-like conditions. They present a model in which the 200–300 μm water emission spectrum is pumped by the absorption of shorter wavelength continuum photons, a scenario supported by absorption measurements with the long-wavelength spectrometer on the *Infrared Space Observatory* (González-Alfonso et al. 2008). The excitation of water is thus coupled closely to the dust continuum intensity, and GA10 are able to use the ISO + SPIRE lines to constrain the size and opacity of the dust continuum source in Mrk 231 between 30 and 150 μm, concluding that it is ~110–180 pc in size.

We might expect to find similar processes at work in the early universe, and our wideband 1 mm surveys with Z-Spec are revealing H_2O in a handful of high-redshift objects (Bradford et al. 2009, hereafter B09; Scott et al. 2010; Omont et al. 2011). We present here a study of APM 08279+5255 at $z = 3.91$, a particularly convenient redshift for characterizing the water emission spectrum in the 1 mm band.

1.2. APM 08279+5255

APM 08279+5255 is an unusual source by any measure. It exhibits an apparent total bolometric luminosity of $7 \times 10^{15}\ L_\odot$,

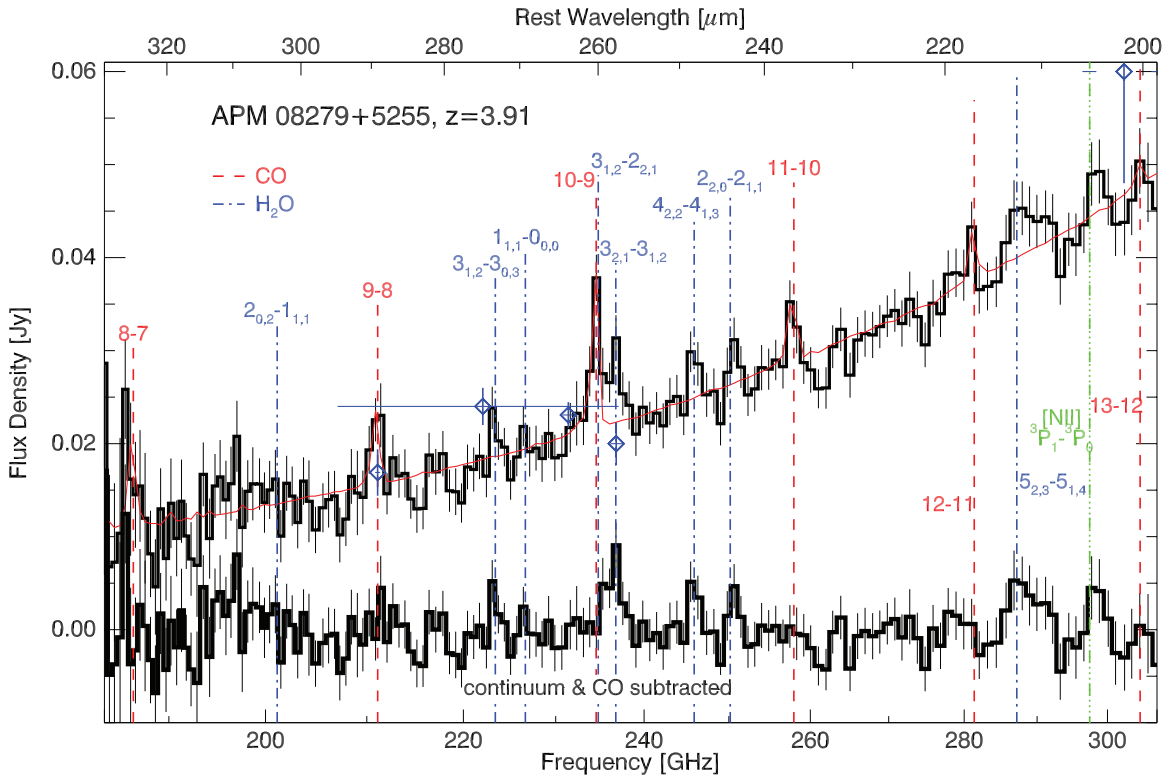

Figure 1. Z-Spec spectrum of APM 08279+5255. Dashed vertical lines show all transitions of CO and H_2O with upper level energies below 700 K, which lie in the band. The position of the [N II] 205 μm transition is also noted. Diamonds show continuum measurements from (in increasing frequency) Plateau de Bure (W07), SCUBA (Lewis et al. 1998), CARMA (this work), CARMA (this work), and the SMA (average of two sidebands—horizontal and vertical bars indicate bandwidth and uncertainty; Krips et al. 2007). The lower spectrum shows the data with a fit to the continuum and CO lines subtracted.

(A color version of this figure is available in the online journal.)

dominated by warm active-galactic-nucleus-heated dust peaking in the rest-frame 15–30 μm regime (Riechers et al. 2009 and references therein, hereafter R09). There is a cold dust component identified in the rest-frame far-IR and submillimeter which contributes ~3% of the total energy. This may be produced by star formation, and the [O III] 88 μm luminosity ($1.06 \times 10^{11}/\mu\ L_\odot$) is consistent with star formation contributing up to ~35% of this far-IR luminosity (Ferkinhoff et al. 2010), or ~1% of the total in the system. APM 08279+5255 has been studied in detail with interferometric observations of CO ranging from $J = 1 \rightarrow 0$ and $J = 2 \rightarrow 1$ with the Very Large Array (VLA; Papadopoulos et al. 2001, more recently by R09) to $J = 11 \rightarrow 10$ with the Plateau de Bure Interferometer (PdB; Weiß et al. 2007, hereafter W07). The compact CO morphology (at least at $J = 1 \rightarrow 0$) is similar to the image of the optical quasar—only just marginally resolved into sub-images at 0.″4—and R09 model the CO $J = 1 \rightarrow 0$-emitting gas as an $R \sim 550$-pc disk, magnified by $\mu = 4$. We adopt this magnification factor, and a luminosity distance of 35,565 Mpc (appropriate for $H_0 = 71$, $\Omega_M = 0.27$, and $\Omega_\Lambda = 0.73$). The W07 CO measurements then translate to an intrinsic molecular gas mass of $M_{\rm total} \sim 1.0 \times 10^{11}\ M_\odot$ using an adopted scale factor of $5.3 \times 10^{11}\ M_\odot\ ({\rm K\,km\,s^{-1}\,pc^2})^{-1}$.

In the R09 lensing model, the magnification is not sharply peaked in the central few hundred parsecs: $\mu(R)$ ranges from 3 to 5 out to source radius $R \sim 10$ kpc. If this is correct, then the CO line ratios and the gas conditions inferred from CO (W07) are largely independent of the lensing, and the high-J CO emission in APM 08279+5255 is particularly unusual among extragalactic sources. To reproduce the ratios among the low-J and high-J CO transitions, W07 require at least two components with conditions ranging from cool and dense ($T \sim 65$ K, $n_{\rm H_2} \sim 1 \times 10^5\ {\rm cm^{-3}}$) to warmer and less dense ($T \sim 225$ K, $n_{\rm H_2} \sim 1 \times 10^4\ {\rm cm^{-3}}$).

2. OBSERVATIONS

APM 08279+5255 was observed with Z-Spec at the Caltech Submillimeter Observatory (CSO) on a total of 13 nights among four observing campaigns: 2008 March 23–28, 2008 April 4–16, 2009 January 6–9, and 2009 February 23–27. We used the chop-and-node mode with a 20 s nod period and a 1.6 Hz, 90″ chop. The total integration time (including chopping) is 25.3 hr, with a range of telluric water vapor burdens; $\tau_{225\,\rm GHz}$ ranged from 0.04 to 0.20, with a median of 0.083 and a mean of 0.102. With all data incorporated in a weighted co-addition, the sensitivity referred to the total integration time ranges from 750 mJy $s^{1/2}$ in the middle of the band (producing a 2.5 mJy channel rms) to 1100 mJy $s^{1/2}$ at the band edges (producing a 3.6 mJy channel rms), with greater degradation below 200 GHz. The data are calibrated using Mars and Uranus, with quasars as secondary calibrators using the method described in B09. Figure 1 shows the spectrum and the line fits described below.

2.1. CARMA Follow-up

The source was also observed using the 15-element Combined Array for Research in Millimeter-wave Astronomy (CARMA; Bock et al. 2006, Figure 2). On 2009 November 9 and 15, with the array in its C configuration, the upper sideband (USB) was tuned to $\nu_{\rm USB} = 236.75$ GHz, corresponding to the H_2O $3_{2,1} \rightarrow 3_{1,2}$ transition at $z = 3.9119$, the redshift measured with PdB for CO $J = 9 \rightarrow 8$ (the highest-J transition measured with the PdB; W07). The lower sideband (LSB) was

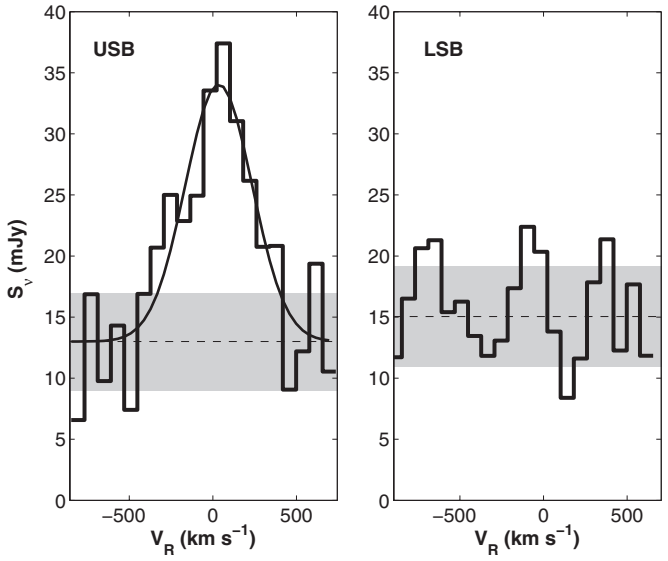

Figure 2. CARMA spectrum of the $3_{2,1} \rightarrow 3_{1,2}$ H_2O transition; the velocity scales refer to $z = 3.9119$. The plotted spectra are not corrected for the atmospheric decorrelation, though the entries in Table 1 are.

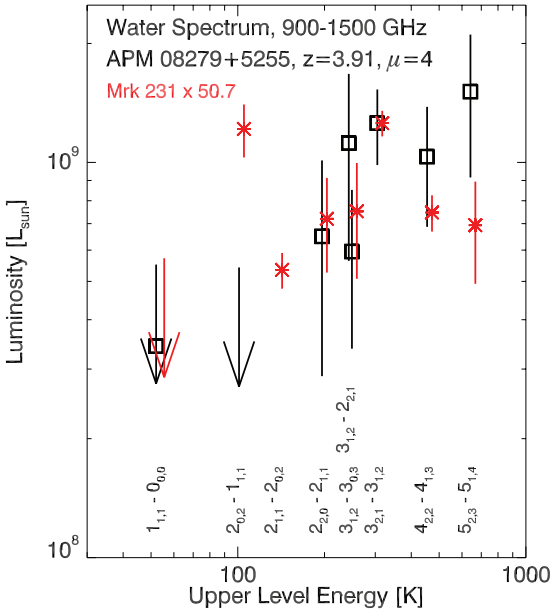

Figure 3. Comparison of the water spectrum in Mrk 231 with that in APM 08279+5255, as measured with Z-Spec. Downward arrows show limits at 2σ. The H_2O $3_{1,2} \rightarrow 2_{2,1}$ flux is not measured in Mrk 231, though as vdW10 note, the $J = 10 \rightarrow 9$ transition likely includes flux from this line.

(A color version of this figure is available in the online journal.)

centered on $\nu_{LSB} = 231.14$ GHz. The correlator was configured in its 3×468.75 MHz setting with partially overlapping windows, yielding an effective coverage of $\Delta\nu \approx 1.3$ GHz ($\Delta v \approx 1600$ km s^{-1}) with a native resolution of ≈31.25 MHz (≈39.6 km s^{-1}).

The double sideband system temperature was $T_{sys} \sim$ 280–480 K, and the total integration time was 9 hr. The quasar 0359+509 was the astronomical bandpass calibrator ($S_\nu \sim 3.5$ Jy), and Mars was the absolute flux calibrator. The quasars 0927+390 ($S_\nu \sim 2.3$ Jy) and 0920+446 ($S_\nu \sim 1.0$ Jy) were the primary and secondary phase calibrators, respectively, on a calibration cycle of 10 minutes. The phase rms on 0927 + 390 after self-calibration was approximately 25°. Atmospheric decorrelation effects were estimated to be 35%, and the fluxes have been corrected accordingly. This is not unexpected since the observations were obtained in a mid-size configuration, with typical baselines of ∼360 m.

The synthesized beam size is $\theta = 0\farcs80 \times 0\farcs64$ with P.A. $= -70\fdg4$. Fitting to the LSB and the USB images are very consistent and suggest that APM 08279+5255 is slightly resolved with an intrinsic angular size of $\theta \approx 0\farcs4$, in agreement with other observations of the source angular size (Krips et al. 2007).

3. RESULTS, CONTINUUM, AND LINE FLUX EXTRACTIONS

A model spectrum consisting of a power-law continuum with 15 Gaussian spectral lines is fit to the 160 bolometer fluxes, incorporating their measured spectral response profiles using the method described in Naylor et al. (2010). The redshift is fixed at 3.9119, and the line width is $\Delta v_{FWHM} = 550$ km s^{-1}. This width is greater than that reported by W07 for the low-J transitions, but is consistent with values measured for the $J = 9 \rightarrow 8$, $J = 10 \rightarrow 9$ CO transitions. In any case, our fits to the Z-Spec spectrum are not very sensitive to the adopted line width. The fitted fluxes and resulting uncertainties are presented in Table 1.

Our CO fluxes are consistent with the W07 IRAM measurements to within the uncertainties, though we do find systematically larger values, e.g., for $J = 9 \rightarrow 8$ and $J = 11 \rightarrow 10$ (35%–45%). Since the continuum measurements are consistent to better than this (see Figure 1), we rule out global calibration problems at this level. It may be that Z-Spec is coupling flux in high-velocity wings of the lines which would be missed in the IRAM spectra, or there could be spatially extended CO emission that the interferometer resolves out. Given the coarse resolution, it is also possible that other transitions near CO are contaminating the Z-Spec fitted flux, though aside from the $J = 10 \rightarrow 9$ transition, there are no significant candidates in the SPIRE Mrk 231 spectrum (van der Werf et al. 2010). In any case, our CARMA measurement is consistent with Z-Spec in both the line flux and continuum to better than the statistical uncertainties.

CO $J = 10 \rightarrow 9$ is clearly blended with the H_2O $3_{1,2} \rightarrow 2_{2,1}$ transition; the two transitions are separated by 297 km s^{-1}, about 1/3 of a Z-Spec channel. We fit the two simultaneously, but only their sum is meaningful. We estimate the flux of CO $J = 10 \rightarrow 9$ as the geometric mean of the $J = 9 \rightarrow 8$ and $J = 11 \rightarrow 10$ intensities in temperature units, and then subtract this value from the fitted flux of the CO+water blend to arrive at an estimate of the flux for the water line. We find that the water and CO fluxes are comparable, though the formal signal-to-noise ratio (S/N) for each is modest (∼2.0) as the errors are propagated in this estimate.

Figure 1 and Table 1 show all eight H_2O transitions in the band with upper level energies less than 700 K. Of these, we detect four in emission with $>2.3\sigma$ significance. While less than the customary 3σ, 2.3σ corresponds to a likelihood of only $(1 - \mathrm{erf}(S/N/\sqrt{2}))/2 = 1.0\%$ that the transition is not real with positive flux, if the noise is Gaussian. In addition to $3_{1,2} \rightarrow 2_{2,1}$ described above (2σ is only 2.2% likely to be false), we tentatively identify two additional transitions in emission at lower significance ($1_{1,1} \rightarrow 0_{0,0}$ and $2_{2,0} \rightarrow 2_{1,1}$) and estimate fluxes and upper limits. $2_{0,2} \rightarrow 1_{1,1}$ can only offer an upper limit. In Figure 3, we plot 2σ upper limits, corresponding to a 98% confidence level.

Table 1
1 mm Line Intensity Measurements in APM 08279+5255

Transition	E_{upper} (K)	ν_{rest} (GHz)	ν_{obs} (GHz)	Flux (Jy km s^{-1})	1σ Err (Jy km s^{-1})[a]	$L_{intrinsic}$ [$10^8 L_\odot$][b]
CO $J=8\rightarrow7$	199	921.80	187.7	12.1	8.3	7.4 ± 5.1
CO $J=9\rightarrow8$	249	1036.91	211.1	16.0	3.8	11.0 ± 2.6
IRAM 30 m (W07)				11.1	2.2	7.7 ± 1.5
IRAM Plateau de Bure (W07)				12.5	2.4	8.6 ± 1.7
CO $J=10\rightarrow9$	304	1151.99	234.6	15.2[c]	7.2	11.6 ± 5.5
IRAM 30 m (W07)				11.9	2.4	9.1 ± 1.8
CO $J=11\rightarrow10$	365	1267.02	258.0	14.4	4.5	12.1 ± 3.8
IRAM 30 m (W07)				10.4	2.1	9.2 ± 1.8
CO $J=12\rightarrow11$	431	1381.00	281.4	9.5	5.0	8.8 ± 4.6
CO $J=13\rightarrow12$	503	1496.92	304.8	4.4	6.1	
H_2O $2_{0,2}\rightarrow1_{1,1}$	101	987.93	201.2	1.9	4.1	<8.1 (3σ)
H_2O $3_{1,2}\rightarrow3_{0,3}$	250	1097.40	223.5	8.1	3.5	5.9 ± 2.6
H_2O $1_{1,1}\rightarrow0_{0,0}$	53.4	1113.34	226.7	4.6	3.7	3.4 ± 2.7 ($3\sigma<8.2$)
H_2O $3_{1,2}\rightarrow2_{2,1}$	250	1153.13	234.8	14.5[c]	7.2	11.1 ± 5.5
H_2O $3_{2,1}\rightarrow3_{1,2}$	305	1162.91	236.8	16.0	3.5	12.4 ± 3.0
CARMA (this work)				16.3	3.5[d]	12.6 ± 2.7
H_2O $4_{2,2}\rightarrow4_{1,3}$	455	1207.64	245.9	12.8	4.3	10.3 ± 4.1
H_2O $2_{2,0}\rightarrow2_{1,1}$	196	1228.79	250.2	7.9	4.4	6.4 ± 4.0 ($3\sigma < 12.0$)
H_2O $5_{2,3}\rightarrow5_{1,4}$	643	1410.62	287.2	16.0	6.3	15.0 ± 5.2
N II $^3P_1 \rightarrow {}^3P_0$	70.1	1461.0	297.4	7.6	5.4	7.4 ± 5.1

Notes.
[a] Z-Spec includes statistical uncertainties only, IRAM uncertainties are ±20%, as per W07.
[b] All luminosities are corrected for lensing, assuming $\mu = 4$.
[c] CO $J=10\rightarrow9$ and H_2O $3_{1,2}\rightarrow2_{2,1}$ are blended, see discussion in the text.
[d] CARMA error dominated by uncertainty in baseline level; the line significance is $\sim13\sigma$.

Measurements from the Plateau de Bure of some of these transitions have recently been made available. Lis et al. (2011) find a flux in the $2_{2,0} \rightarrow 2_{1,1}$ transition which matches ours to within 0.3σ. van der Werf et al. (2011) report fluxes of three other transitions in the Z-Space band. They detect $2_{0,2} \rightarrow 1_{1,1}$ finding a flux consistent with our measurement and our 1σ uncertainty. They find the $3_{2,1} \rightarrow 3_{1,2}$ transition with a flux 1.7σ lower than our measurement ($\sim2\sigma$), a discrepancy similar to but slightly larger than that noted above for the CO transitions. The greatest discrepancy is in the $4_{2,2} \rightarrow 4_{1,3}$ transition, for which they find a factor of 5 lower flux. This discrepancy is inconsistent with errors in either measurement. The formal uncertainties with Z-Spec are of course much higher, but the very small velocity width in the PdB spectrum is difficult to understand. We are undertaking further observations with CARMA to resolve this discrepancy.

The ground-state fine-structure transition of [N II] ($^3P_1 \rightarrow {}^3P_0$, $\lambda_{rest} = 205.18\ \mu$m) is identified as tentatively in emission at low significance (1.4σ). The value is consistent with the lower limit obtained by Krips et al. (2007) with the Submillimeter Array (SMA; $3\sigma < 9$ Jy km s^{-1} in a single beam, $3\sigma < 16$ Jy km s^{-1} if scaled to the continuum source size; Ferkinhoff et al. 2010).

4. ANALYSIS AND DISCUSSION

4.1. CO Emission and XDR Heating

We find that the ratios among the high-J CO transitions are consistent with the excitation model presented in W07. If the IRAM fluxes are increased to match the Z-Spec values with the factor of 1.4 described above, our $J = 8 \rightarrow 7$ and $J = 12 \rightarrow 11$ fluxes and the $J = 13 \rightarrow 12$ limit all fall on the CO excitation curves in Figures 7 and 9 of W07, matching to well within the statistical uncertainties. We estimate a total lensing-corrected CO luminosity of $\sim 7 \times 10^9\ L_\odot$, a fraction 1.4×10^{-4} of the $5 \times 10^{13}\ L_\odot$ output in the far-IR per the decomposition of R09. This total CO luminosity fraction is not unusually high; it is comparable to the value in local starburst galaxies and ULIRGs for which the spectra have now been measured with Herschel SPIRE. L_{CO}/L_{IR} is 1.25×10^{-4} in M82 (Panuzzo et al. 2010), 1.0×10^{-4} in Arp 220 (Rangwala et al. 2011), and 7×10^{-5} in Mrk 231 (vdW10). However, as W07 have noted, the CO excitation of APM 08279+5255 is much higher: the $J = 11 \rightarrow 10$ to $J = 6 \rightarrow 5$ luminosity ratio, for example ranges from 0.54 ± 0.13 in M82 to ~1 in Mrk 231 to 2.5–3.5 in APM 08279+5255, depending on the calibration. Since the high-lying CO transitions in Mrk 231 cannot be understood in a reasonable photo-dissociation region (PDR) framework, the even more extreme ratios in APM 08279+5255 cannot be fit by PDR models either.

Given the powerful hard X-ray source, it is likely the high-J CO emission is due to gas cooling in X-ray dominated regions (XDRs; Maloney et al. 1996), as has been modeled for both Mrk 231 and the Cloverleaf system (B09). For APM 08279+5255, we estimate an intrinsic 1–100 keV luminosity of 1×10^{46} erg s^{-1} by extrapolating the apparent luminosity in the rest-frame 2–10 keV range of 2.3×10^{46} erg s^{-1} as per Just et al. (2007). This is similar to the hard X-ray luminosity inferred for the Cloverleaf, and if we assume the same attenuating column of $N_{H,att} = 3 \times 10^{23}$ cm^{-3} (as is required to maintain a molecular phase), then we can use the same model as in B09 to consider the CO excitation (Figures 6–8 in B09). Assuming the CO emission emerges from a 550-pc disk as per R09, then the CO surface brightness (erg s^{-1} cm^{-2}) in APM 08279+5255 is 0.7–0.8 erg s^{-1} cm^{-2}, some 3.5–4 times that of the Cloverleaf. This emergent flux is readily produced with $R < 650$ pc and $n_H > 2 \times 10^5$ cm^{-3} ($n_{H_2} > 1 \times 10^5$ cm^{-3} if fully molecular). The

required density is on the high end of that inferred in the W07 CO analysis, but this is overall a good match to the observed parameters.

4.2. Water Emission and Radiative Pumping

Considering the available transitions in our band, we find a total luminosity of $6.5\times10^9\ L_\odot$ in the water rotational network. This is a lower bound, but is already close to the total CO emission, suggesting that water is energetically important to the gas. As GA10 found for Mrk 231, the ratio of luminosity in the high-excitation transitions relative to the low-lying ones indicates that the high-excitation levels are not excited collisionally. The conditions inferred by W07 using CO (temperature from 70 to 200 K and n_{H_2} between 10^4 and $10^5\ \mathrm{cm}^{-3}$) are well below even the extreme conditions considered by GA10 ($T = 200$ K, $n_{H_2} = 1.5\times10^6\ \mathrm{cm}^{-3}$) in considering collisional excitation.

Figure 3 shows a comparison of the APM 08279+5255 H_2O spectrum to that of Mrk 231 (adopting $d_L = 184$ Mpc). To our measurement accuracy, the emission in the high-lying lines in APM 08279+5255 resembles that in Mrk 231, scaled up by $\sim$50×. In fact, APM 08279+5255 shows an even higher ratio of the $E_{upper} > 200$ K transitions to the lower energy ones. There is plenty of molecular material in the source—the R09 molecular gas mass estimate is a factor of 22 times the GA10 estimate for Mrk 231, including all three components, but it is some 300× the modeled warm component which dominates the high-lying water emission in Mrk 231. Thus, even modest water abundance throughout, or an abundance similar to that obtained in Mrk 231 in 1/6 of the total gas reservoir would be sufficient to produce the observed luminosity in APM 08279+5255, if it is suitably excited.

The low significance of the detections and lack of higher frequency coverage for the absorption transitions do not warrant a detailed radiative transfer model, but it is easy to show that the powerful dust continuum in APM 08279+5255 can readily pump the observed water transitions with the same mechanism as that modeled by GA10 for Mrk 231. Assuming spherical symmetry, the observed flux constrains the size of a fiducial region R_s around a dust-emitting source via

$$(\nu F_\nu)_{\rm obs}\ \mu^{-1} = \frac{(\nu L_\nu)_{\rm em}}{4\pi d_L^2} = \frac{R_s^2}{d_L^2}\,\nu_{\rm em}\int I_{\nu\,\rm em}\,d\Omega, \qquad (1)$$

where d_L is the luminosity distance and μ is the magnification factor. $I_\nu(\Omega)$ is the specific intensity produced by the dust distribution; it captures brightness temperature and opacity as a function of viewing angle. For a pumping transition at $\nu_{\rm em}$ this integral of I_ν over a solid angle is the quantity that sets the pumping rate per molecule in a given transition. Holding this constant allows an estimate of the ratio of the size scale over which similar pump conditions like those in Mrk 231 exist in APM 08279+5255, through the scaling

$$R_s \propto d_L[(\nu F_\nu)_{\rm obs}\mu^{-1}]^{1/2}, \qquad (2)$$

giving

$$V_w \propto R_s^3 \propto d_L^3[(\nu F_\nu)_{\rm obs}\mu^{-1}]^{3/2}. \qquad (3)$$

As an example, we consider pumping of the $3_{1,3}$ level with absorption at 58 μm, producing the $4_{2,2}\rightarrow4_{1,3}$ transition in emission. Given the observed fluxes, the scaling above suggests that R_s is 5.1 times larger for APM 08279+5255 than for Mrk 231. For similar geometries, then, the continuum-emitting source in APM 08279+5255 is capable of illuminating a volume $\sim R_s^3 \sim 130$ times larger than Mrk 231 with a similar pump rate. This is a reasonable match to the factor of 50–90 larger luminosity in this transition in APM 08279+5255. We expect that for APM 08279+5255, the higher color temperature would preferentially pump via higher frequency far-IR transitions relative to Mrk 231, and this likely explains the increased flux in the $5_{2,3}\rightarrow5_{1,4}$ transition (pumped via 45 μm) and the reduced flux in $3_{1,2}\rightarrow2_{2,1}$ (pumped via 75 μm).

The Mrk 231 warm water-emitting component is modeled by GA10 as a sphere of dust and gas of size 110–180 pc. With the above scaling, we know that similar pump conditions must exist in APM 08279+5255 out to distances of 560–920 pc. This may seem extreme, but APM 08279+5255 is an extremely powerful system; consider that the smallest possible physical size for the 220 K source is in the limit of an optically thick (at $\lambda_{\rm peak}$) sphere, for which $R_{\rm min} \sim 215$ pc. Thus, if the molecular gas is really situated in a $R \sim 550$-pc disk as per the model of R09, then a large fraction of the molecular mass in this system is capable of being pumped to the level of the warm component in the Mrk 231 model. Indeed, the simple model suggests that the water must exist at such large distances because the system is so opaque. If we require that the same 220 K, 215-pc dust component account for the emission at $\lambda_{\rm rest} = 250\,\mu$m, then it must have an opacity of $\sim$0.8 at this wavelength. Any contribution from a lower temperature material requires a combination of larger opacity and/or larger physical size. In the spherically symmetric model then, this indicates either that the observed fluxes in the water lines must be extinction corrected with large factors, or more likely, that most of the observed line emission originates at $R \geqslant 200$ pc. This interpretation is consistent with that of Srianand & Petitjean (2000) who find that radiative excitation from a far-IR source larger than the UV source, and at least 200 pc, is required to explain the presence of [Si II] and [C II] in the upper far-IR levels indicated in optical absorption studies.

Without more detailed geometric constraints, we can only conclude that the total mass of water vapor is at least $\sim$50 times that of Mrk 231, some $2.5\times10^4\ M_\odot$, and is likely distributed over scales larger than 200 pc, comparable to the 550-pc size scale inferred from the CO imaging. The mass of water vapor corresponds to an average abundance relative to H_2 of $\geqslant1.4\times10^{-7}$, when referred to the full molecular gas mass in APM 08279+5255. This estimate is a good match to our XDR model, which predicts a water abundance of $(1.4\text{–}2.0)\times10^{-7}$ with the parameters described above.

We are indebted to the staff of the Caltech Submillimeter Observatory for their help in Z-Spec's commissioning and observing. We acknowledge the following grants and fellowships: NASA SARA grants NAGS-11911 and NAGS-12788, NSF AST grant 0807990, an NSF Career grant (AST-0239270) and a Research Corporation Award (RI0928) to J. Glenn, a Caltech Millikan and JPL Director's fellowships to C.M.B., an NRAO Jansky fellowship to J. E. Aguirre, NASA GSRP fellowship to L. Earle, and an NSF GSRP award to J. Kamenetzky. The research described in this Letter, carried out at the Jet Propulsion Laboratory, California Institute of Technology, was done under a contract with the National Aeronautics and Space Administration.

REFERENCES

Bock, D. C.-J., Bolatto, A. D., Hawkins, D. W., et al. 2006, Proc. SPIE, 6267, 626713

Bradford, C. M., Aguirre, J. E., Aikin, R., et al. 2009, ApJ, 705, 112 (B09)

Cernicharo, J., Goicoechea, J. R., Daniel, F., et al. 2006, ApJ, 649, L33
Draine, B. T., & Roberge, W. G. 1982, ApJ, 259, L91
Earle, L., Ade, P., Aguirre, J., et al. 2006, Proc. SPIE, 6275, 627510
Ferkinhoff, C., Hailey-Dunsheath, S., Nikola, T., et al. 2010, ApJ, 714, L147
Fixsen, D. J., Bennett, C. L., & Mather, J. C. 1999, ApJ, 526, 207
González-Alfonso, E., Fischer, J., Isaak, K., et al. 2010, A&A, 518, L43 (GA10)
González-Alfonso, E., Smith, H. A., Ashby, M. L. N., et al. 2008, ApJ, 675, 303
Griffin, M. J., Abergel, A., Abreu, A., et al. 2010, A&A, 518, L3
Hollenbach, D., & McKee, C. F. 1979, ApJS, 41, 555
Just, D. W., Brandt, W. N., Shemmer, O., et al. 2007, ApJ, 665, 1004
Krips, M., Peck, A. B., Sakamoto, K., et al. 2007, ApJ, 671, L5
Lewis, G. F., Chapman, S. C., Ibata, R. A., Irwin, M. J., & Totten, E. J. 1998, ApJ, 505, L1
Lis, D. C., Neufeld, D. A., Phillips, T. G., Gerin, M., & Neri, R. 2011, ApJ, 738, L6
Maloney, P. R., Hollenbach, D. J., & Tielens, A. G. G. M. 1996, ApJ, 466, 561
Naylor, B. J., Bradford, C. M., Aguirre, J. E., et al. 2010, ApJ, 722, 668
Neufeld, D. A., & Kaufman, M. J. 1993, ApJ, 418, 263
Neufeld, D. A., & Melnick, G. J. 1987, ApJ, 322, 266
Omont, A., Neri, R., Cox, P., et al. 2011, A&A, 530, L3
Panuzzo, P., Rangwala, N., Rykala, A., et al. 2010, A&A, 518, L37
Papadopoulos, P., Ivison, R., Carilli, C., & Lewis, G. 2001, Nature, 409, 58
Rangwala, N., Maloney, P. R., Glenn, J., et al. 2011, ApJ, in press (arXiv:1106.5054)
Riechers, D. A., Walter, F., Carilli, C. L., & Lewis, G. F. 2009, ApJ, 690, 463 (R09)
Scott, K. S., Lupu, R. E., Aguirre, J. E., et al. 2010, ApJ, in press (arXiv:1104.4115)
Scoville, N. Z., & Kwan, J. 1976, ApJ, 206, 718
Srianand, R., & Petitjean, P. 2000, A&A, 357, 414
van der Werf, P. P., Berciano Alba, A., Spaans, M., et al. 2011, ApJ, 741, L38
van der Werf, P. P., Isaak, K. G., Meijerink, R., et al. 2010, A&A, 518, L42 (vdW10)
Weiß, A., Downes, D., Neri, R., et al. 2007, A&A, 467, 955 (W07)